# The 'KMSKS' Motif in Tyrosyl-tRNA Synthetase Participates in the Initial Binding of $tRNA^{Tyr}$†

Yu Xin, Weidong Li, and Eric A. First*

*Department of Biochemistry and Molecular Biology, Louisiana State University Medical Center in Shreveport, Shreveport, Louisiana 71130*

*Received July 20, 1999; Revised Manuscript Received November 2, 1999*

ABSTRACT: Variants at each position of the 'KMSKS' signature motif in tyrosyl-tRNA synthetase have been analyzed to test the hypothesis that this motif is involved in catalysis of the second step of the aminoacylation reaction (i.e., the transfer of tyrosine from the enzyme-bound tyrosyl-adenylate intermediate to the $tRNA^{Tyr}$ substrate). Pre-steady-state kinetic studies show that while the rate constants for tyrosine transfer ($k_4$) are similar to the wild-type value for all of the mobile loop variants, the K230A and K233A variants have increased dissociation constants ($K_d^{tRNA}$ = 2.4 and 1.7 $\mu$M, respectively) relative to the wild-type enzyme ($K_d^{tRNA}$ = 0.39 $\mu$M). In contrast, the $K_d^{tRNA}$ values for the F231L, G232A, and T234A variants are similar to that of the wild-type enzyme. The $K_d^{tRNA}$ value for a loop deletion variant, Δ(227−234), is similar to that for the K230A/K233A double mutant variant (3.4 and 3.0 $\mu$M, respectively). Double mutant free energy cycle analysis indicates there is a synergistic interaction between the side chains of K230 and K233 during the initial binding of $tRNA^{Tyr}$ ($\Delta\Delta G_{int}$ = −0.74 kcal/mol). These results suggest that while the 'KMSKS' motif is important for the initial binding of $tRNA^{Tyr}$ to tyrosyl-tRNA synthetase, it does not play a catalytic role in the second step of the reaction. These studies provide the first kinetic evidence that the 'KMSKS' motif plays a role in the initial binding of $tRNA^{Tyr}$ to tyrosyl-tRNA synthetase.

The aminoacyl-tRNA synthetases (AARS)[1] catalyze the aminoacylation of tRNA by the following two-step reaction:

$$\text{AARS} + \text{AA} + \text{ATP} \rightleftarrows \text{AARS}\cdot\text{AA-AMP} + \text{PP}_i \quad (1)$$

$$\text{AARS}\cdot\text{AA-AMP} + \text{tRNA}^{AA} \rightleftarrows \text{AARS} + \text{AMP} + \text{AA-tRNA}^{AA} \quad (2)$$

In the first step of the reaction, the amino acid is activated by ATP to form an enzyme-bound aminoacyl-adenylate intermediate (AARS·AA-AMP). In the second step of the reaction, the amino acid is transferred to its cognate tRNA ($tRNA^{AA}$), and the aminoacyl-tRNA ($AA\text{-}tRNA^{AA}$) and AMP products are released from the enzyme. Aminoacyl-tRNA synthetases can be divided into two distinct classes on the basis of their structural architecture (*1*, *2*). Class I aminoacyl-tRNA synthetases have a common Rossmann fold domain and characteristic 'HIGH' and 'KMSKS' signature motifs (*3*−*10*). The 'KMSKS' signature motif corresponds to the "Walker" sequence found in a number of other nucleotide binding proteins (*11*, *12*). Class II aminoacyl-tRNA synthetases are characterized by a six-stranded antiparallel $\beta$-sheet packed between two long α-helices (*13*). They possess three conserved sequence motifs, with motif 1 (+GΦXXΦXλPΦΦ) forming part of the dimer interface, and motif 2 (+ΦΦXΦλXXFRXEX$_{n=4-12}$+ΦXXFXX-F) and motif 3 (λXΦGΦGΦGΦERΦΦΦΦΦ)[2] containing active site residues that are critical for catalysis (*1*, *13*, *14*).

Tyrosyl-tRNA synthetase belongs to the Class I aminoacyl-tRNA synthetase family. Tyrosyl-tRNA synthetase from *Bacillus stearothermophilus (B. stearothermophilus)* is a dimeric enzyme composed of two identical 47 kDa monomers (*5*). Although there are two active sites per dimer, tyrosyl-tRNA synthetase exhibits half-of-sites reactivity with respect to the binding of tyrosine and formation of the enzyme-bound tyrosyl-adenylate intermediate (*15*−*19*). In tyrosyl-tRNA synthetase, the actual amino acid sequence of the 'KMSKS' motif is '$K_{230}$FGK$T_{234}$'. Previous studies have shown that the mobile loop containing amino acids K230 through T234 in tyrosyl-tRNA synthetase stabilizes the pyrophosphate moiety of the transition state complex for the first step of the aminoacylation reaction. Three amino acid residues in the mobile loop, K230, K233, and T234, were shown to be responsible for this effect (*20*−*24*). In this study, we test the hypothesis that amino acids K230, K233, and T234 in tyrosyl-tRNA synthetase stabilize the transition state complex for the second step of the aminoacylation reaction. This hypothesis is based on several lines of evidence. All of the above amino acid residues are located on a mobile loop in tyrosyl-tRNA synthetase and, due to their involvement in the first step of the reaction, are known to be in the vicinity

† This work is supported by National Institutes of Health Grant GM53693.

* To whom correspondence should be addressed. Tel: 318-675-7779; Fax: 318-675-5180; E-mail: efirst@lsumc.edu.

[1] Abbreviations: AA, amino acid(s); AARS, aminoacyl-tRNA synthetase(s); $PP_i$, pyrophosphatase; "-", covalent bond; "·", noncovalent bond; AARS·AA-AMP, enzyme-bound aminoacyl-adenylate; $AA\text{-}tRNA^{AA}$, aminoacyl-tRNA; TyrRS, tyrosyl-tRNA synthetase.

[2] +, a positively charged amino acid (H, K, R); Φ, a hydrophobic amino acid (I, L, M, F, W, or V); λ, a small amino acid (A, C, G, P, S, or T); −, a negatively charged amino acid (D, N, E, Q); X, any amino acid. Class II invariant amino acid residues are underlined.

10.1021/bi991675l CCC: $19.00 
Published on Web 12/17/1999

of both the $\beta$- and $\gamma$-phosphates of ATP and, presumably, the 3′ end of $tRNA^{Tyr}$ (*20*−*24*). In addition, periodate oxidation of $tRNA^{Tyr}$ has been shown to form covalent cross-links with two lysines in the '$K_{230}FGKT_{234}$' sequence of tyrosyl-tRNA synthetase, as well as with the nonconserved lysine (K225) preceding this sequence (*3*). Finally, the high degree of sequence conservation of the 'KFGKT' sequence among Class I aminoacyl-tRNA synthetases raises the possibility that this sequence plays a catalytic role in both steps of the aminoacylation reaction and, in particular, interacts with the invariant adenosine 76 of the tRNA substrate. To test the hypothesis that the 'KFGKT' sequence in tyrosyl-tRNA synthetase stabilizes the transition state complex for the second step of the aminoacylation reaction, we investigated the effects that mutation of each amino acid residue in the '$K_{230}FGKT_{234}$' sequence has on the binding of $tRNA^{Tyr}$ and stabilization of the transition state complex for the second step of the aminoacylation reaction. Pre-steady-state kinetic methods are used to monitor the transfer of tyrosine to $tRNA^{Tyr}$ independently of the first step of the reaction (i.e., tyrosine activation). In addition, double mutant free energy cycles are used to analyze the role that pairwise coupling between the side chains of K230 and K233 plays in the catalysis of the second step of the $tRNA^{Tyr}$ aminoacylation reaction. The results of these analyses provide the first kinetic evidence that the 'KFGKT' sequence plays a role in the initial binding of $tRNA^{Tyr}$ to tyrosyl-tRNA synthetase.

## EXPERIMENTAL PROCEDURES

*Materials.* Reagents were purchased from the following sources: NuSieve low melting point agarose (FMC BioProducts), L-[$^{14}$C]tyrosine (Moravek Biochemicals), [$\gamma$-$^{32}$P]-GTP (ICN Biomedicals Inc.), UTPαS (New England Biolabs), [5′-$^{32}$P]-pCp (ICN Biomedicals Inc.), nitrocellulose filters (Schleicher & Schuell), T4 RNA ligase (New England Biolabs), RNases T1 and U2 (Amersham), RNasin (Promega), and inorganic pyrophosphatase (Sigma). T7 RNA polymerase was expressed as recombinant protein in *Escherichia coli* (*E. coli*) and purified as described by Avis et al. (*27*). Automated DNA sequencing was performed by the DNA sequencing facility at Iowa State University using dye-labeled dideoxy terminators. All other chemicals and reagents were purchased from Fisher Scientific.

*In Vitro Mutagenesis and Purification of the Wild-Type and Variant Tyrosyl-tRNA Synthetases*. The construction of the wild-type and variant tyrosyl-tRNA synthetases used in these studies has been previously described (*21*, *22*).

Purification of the wild-type and variant tyrosyl-tRNA synthetases was performed as previously described (*20*−*24*). Briefly, the purification consists of the following: (1) expression of tyrosyl-tRNA synthetase in *E. coli* TG2 cells (*25*); (2) lysis of the *E. coli* cells and incubation of the extract at 56 °C for 40 min, followed by centrifugation to remove the *E. coli* tyrosyl-tRNA synthetase, as well as other contaminating *E. coli* proteins; (3) dialysis of the remaining supernatant against three changes of 20 mM Tris, pH 7.78, 1 mM EDTA, 5 mM $\beta$-mercaptoethanol buffer containing 0.1 mM pyrophosphate to remove any tyrosyl-adenylate bound to the tyrosyl-tRNA synthetase, followed by dialysis against 20 mM Bistris, pH 6.0, 1 mM EDTA, 5 mM $\beta$-mercaptoethanol; and (4) HPLC purification of the *B. stearothermophilus* tyrosyl-tRNA synthetase variants on a BioRad UNO Q6 anion exchange column using a gradient from 20 mM Bistris, pH 6.0, to 20 mM Bistris, pH 6.0, 1 M NaCl. A peak eluting at 200 mM NaCl was collected and dialyzed overnight against 20 mM Tris, pH 7.78, 1 mM EDTA, 5 mM $\beta$-mercaptoethanol. This protein was then repurified on a BioRad UNO Q6 column using a gradient from 20 mM Tris, pH 7.78, to 20 mM Tris, pH 7.78, 1 M NaCl. A peak eluting at 220 mM NaCl was collected and dialyzed overnight against 20 mM Tris, pH 7.78, 1 mM EDTA, 5 mM $\beta$-mercaptoethanol, and 10% glycerol (v/v). Purified protein was stored at −70 °C. A single band corresponding to the *B. stearothermophilus* tyrosyl-tRNA synthetase was observed on SDS−polyacrylamide gel electrophoresis. The concentration of the tyrosyl-tRNA synthetase was determined using a filter-based active-site titration assay, in which the incorporation of [$^{14}$C]tyrosine into the enzyme-bound tyrosyl-adenylate intermediate is monitored (*26*). Briefly, tyrosyl-tRNA synthetase was incubated with 10 mM ATP and 50 $\mu$M [$^{14}$C]tyrosine for 5 min at 25 °C. Aliquots were then removed from the reaction and passed through nitrocellulose filters, which retained the [$^{14}$C]-tyrosine bound in the tyrosyl-tRNA synthetase·Tyr-AMP complex, but not the free [$^{14}$C]tyrosine.

*In Vitro Transcription of the $tRNA^{Tyr}$ Substrate*. The $tRNA^{Tyr}$ substrate was prepared by in vitro transcription of *Fok*I-linearized pGFX-WT plasmid, which contains the coding sequence of *B. stearothermophilus* $tRNA^{Tyr}$ immediately downstream from a T7 RNA polymerase promoter and immediately upstream from a *Fok*I site [pGFX-WT is a derivative of the pGAG2 plasmid described by Avis et al. (*27*)]. In vitro transcription of $tRNA^{Tyr}$ was performed using a modification of the procedure described by Avis et al. (*27*). A typical 5 mL reaction contained 200 mM HEPES, pH 7.5, 20 mM $MgCl_2$, 40 mM dithiothreitol, 4 mM spermidine, 100 $\mu$g/mL bovine serum albumin, 6.25 mM each NTP, 10 mM GMP, 0.06 mg/mL *Fok*I-linearized pGFX-WT plasmid, 200 units/mL RNasin, 0.4 unit/mL pyrophosphatase, and 0.3 mg/mL T7 RNA polymerase. The addition of GMP to the in vitro transcription reaction results in $tRNA^{Tyr}$ that contains a single phosphate group on the 5′-terminal guanosine. In vitro transcribed $tRNA^{Tyr}$ was purified by extraction with a phenol/chloroform/isoamyl alcohol mixture (25:24:1) as described in Avis et al. (*27*), followed by separation on a $C_4$ reverse-phase column (Phenomenex) using a gradient from 10 mM $MgCl_2$, 10 mM sodium phosphate, pH 5.5, 1 M sodium formate (buffer A), to 10 mM sodium phosphate, pH 5.5, and 10% methanol (v/v) (buffer B) (*28*, *29*). A peak eluting at 35% buffer B was ethanol precipitated and resuspended in 10 mM $MgCl_2$. The sample was annealed by incubation at 80 °C for 15−20 min, followed by slow cooling over the course of 4 h, until the sample reached room temperature. A nitrocellulose filter assay, in which the incorporation of [$^{14}$C]tyrosine into the Tyr-$tRNA^{Tyr}$ product is monitored, was used to determine the concentration of $tRNA^{Tyr}$. In this assay, tyrosyl-tRNA synthetase is preincubated with 10 mM ATP and 50 $\mu$M [$^{14}$C]tyrosine at 25 °C for 5 min. The substrate $tRNA^{Tyr}$ is then added; 10 $\mu$L aliquots are removed from the reaction at various time points, quenched by the addition of 5% TCA, and then passed through nitrocellulose filters, which retains the [$^{14}$C]tyrosine bound in the Tyr-$tRNA^{Tyr}$ complex, but not free [$^{14}$C]tyrosine.

Greater than 95% of the $tRNA^{Tyr}$ sample was aminoacylated as judged by comparison of the $tRNA^{Tyr}$ concentration calculated from the absorbance at 260 nm with the concentration calculated from [$^{14}$C]tyrosine incorporation into the Tyr-$tRNA^{Tyr}$ product.

The 3′ and 5′ termini of the in vitro transcribed $tRNA^{Tyr}$ sample were analyzed to verify that they were intact and homogeneous. The $tRNA^{Tyr}$ sample used for these analyses was prepared without the addition of GMP in the in vitro transcription reaction. Analysis of the 5′ end of $tRNA^{Tyr}$ was performed as described by Pleiss et al. (*30*). Briefly, [$\gamma$-$^{32}$P]-GTP at a specific activity of 1000 Ci/mol was added to the in vitro transcription reaction. Phosphorothioate incorporation was accomplished by substituting UTP with 4 mM UTP$\alpha$S in the in vitro transcription reaction. After 4 h at 37 °C, the reaction was quenched by addition of 10 volumes of 300 mM sodium acetate, 0.5 mM EDTA, and then purified on a NAP 25 column (Pharmacia) preequilibrated in the same buffer. The samples were precipitated with 3 volumes of 95% ethanol. A solution containing 1 mM iodine, 10 mM Tris, pH 8.0, and 10% ethanol was used to cleave the phosphorothioate-containing $tRNA^{Tyr}$. After 5 min at room temperature, the reaction was quenched by addition of sodium bisulfite to a final concentration of 10 mM. The products of the cleaved and uncleaved $tRNA^{Tyr}$ substrates were analyzed on a 45 cm 12% polyacrylamide sequencing gel. Uncleaved $tRNA^{Tyr}$ ran as a single band in the sequencing gel. Greater than 90% of the $tRNA^{Tyr}$ products had homogeneous 5′ ends as judged by the absence of bands with inappropriate gel mobilities (i.e., bands that did not correspond to the predicted iodine cleavage products).

The 3′ end of the $tRNA^{Tyr}$ was labeled by using $T_4$ RNA ligase and [5′-$^{32}$P]-pCp (*31*). Analysis of the 3′ end of the $tRNA^{Tyr}$ was performed using limited RNase T1 and U2 nuclease digestion (*32*). The products of the cleaved $tRNA^{Tyr}$ substrates were analyzed on a 45 cm 12% polyacrylamide sequencing gel. Greater than 90% of the $tRNA^{Tyr}$ sample showed homogeneous 3′ ends.

*Steady-State Fluorescence Spectra of the Tyrosyl-tRNA Synthetase·Tyr-AMP Intermediate*. Changes in the steady-state fluorescence spectra of the tyrosyl-tRNA synthetase·Tyr-AMP intermediate (E·Tyr-AMP) on the addition of $tRNA^{Tyr}$ were quantified using a Proton Technology International TimeMaster Fluorescence Spectrometer. Corrections for inner filter effects, resulting from the addition of $tRNA^{Tyr}$ to the sample, were performed as described by Avis et al. (*27*). Briefly, this involves normalizing the changes in fluorescence due to the $tRNA^{Tyr}$ substrate to a control sample in which nonspecific yeast tRNA has been added at the same absorbance as the $tRNA^{Tyr}$ substrate. The normalized fluorescence value is calculated using the following equation:

$$\Delta F_{norm} = \frac{F_{control} - F_{sample}}{F_{control}} \quad (3)$$

*In Vitro Analysis of the Tyrosyl-tRNA Synthetase Variants: Pre-Steady-State Kinetic Measurements of $tRNA^{Tyr}$ Aminoacylation*. Pre-steady-state kinetic measurements were used to study the second step of the aminoacylation reaction. Pre-steady-state kinetics for the $tRNA^{Tyr}$ aminoacylation reaction were followed by monitoring the changes in the intrinsic protein fluorescence of the tyrosyl-tRNA synthetase at 295 nm, using a stopped-flow fluorescence assay in which in vitro transcribed $tRNA^{Tyr}$ was used as the substrate (an Applied Photophysics model SX 18.MV stopped-flow spectrophotometer was used for these experiments) (*27*). The E·Tyr-AMP intermediate was preformed by incubating tyrosyl-tRNA synthetase with 10 mM Mg·ATP and 100 $\mu$M tyrosine at 25 °C for 30−45 min (*27*). The E·Tyr-AMP intermediate was then isolated by chromatography on a NAP 25 column (Pharmacia) (*27*). This complex was mixed with various concentrations of in vitro transcribed $tRNA^{Tyr}$ substrate in the stopped-flow fluorometer, and the change in the intrinsic fluorescence of the protein was monitored over time. The forward rate constant ($k_4$) for the transfer of tyrosine to $tRNA^{Tyr}$ and the dissociation constant for the dissociation of $tRNA^{Tyr}$ from the enzyme-bound tyrosyl-adenylate intermediate ($K_d^{tRNA}$) were calculated from the dependence of the initial reaction rate on the $tRNA^{Tyr}$ concentration (*27*). Since the inner filter effect on the intrinsic fluorescence of tyrosyl-tRNA synthetase is constant throughout the course of the reaction, it can be neglected during the initial reaction rate calculations.

*Calculation of Free Energies of Binding*. The following equations were used to calculate the free energies for the E·Tyr-AMP·$tRNA^{Tyr}$ and E·[Tyr-$tRNA^{Tyr}$·AMP]$^{‡}$ complexes (*27*):

$$\Delta G_{E\cdot Tyr-AMP\cdot tRNA} = RT \ln K_d^{tRNA} \quad (4)$$

$$\Delta G_{E\cdot[Tyr-tRNA\cdot AMP]^{‡}} = RT \ln(k_B T/h) - RT \ln(k_4/K_d^{tRNA}) \quad (5)$$

where E·Tyr-AMP·$tRNA^{Tyr}$ is an intermediate complex preceding the formation of the transition state for the second step of the $tRNA^{Tyr}$ aminoacylation reaction, E·[Tyr-$tRNA^{Tyr}$·AMP]$^{‡}$ is the transition state complex, $k_B$ is Boltzmann's constant, $T$ is the absolute temperature in degrees kelvin, $h$ is Planck's constant, and $R$ is the gas constant. Free energies were calculated relative to the free energy for the E·Tyr-AMP complex.

*Analyzing the Synergistic Coupling between K230 and K233*. Double mutant free energy cycle analysis was used to investigate the specific interactions between amino acid side chains during catalysis as described previously (*24*, *33*−*35*). The theoretical basis for this strategy is as follows. Consider the free energy cycle shown in Figure 1, involving the mutation of two wild-type amino acids (denoted by K230 and K233) to alanine residues (denoted by K230A and K233A). In this figure, the reference state for the enzyme is defined to be the double mutant (K230A, K233A). For the K230A, K233A → K230A, K233 transition, $\Delta G_a$ is the free energy change that corresponds to the introduction of a lysine side chain at position 233 in the absence of a lysine side chain at position 230. For the K230, K233A → K230, K233 transition, however, the free energy change ($\Delta G_d$) corresponds to the introduction of a lysine side chain at position 233 in the presence of a lysine side chain at position 230. $\Delta G_d$ is thus composed of two terms: (1) a term corresponding to the introduction of amino acid K233 in the absence of the K230, K233 interaction (i.e., $\Delta G_a$); and (2) a term corresponding to the interaction between the side chains of amino acids K230 and K233 ($\Delta\Delta G_{int}$). In mathematical

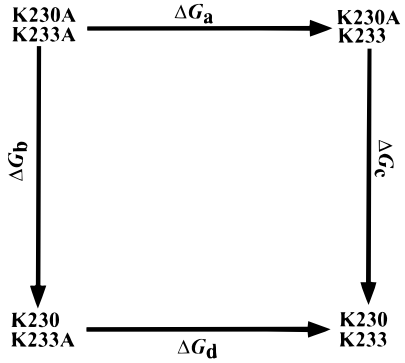


FIGURE 1: Double mutant free energy cycle involving the replacement of two alanine side chains (indicated by K230A, K233A) by the side chains found in the wild-type enzyme, K230 and K233 (i.e., K230A, K233A is the double mutant and K230, K233 is the wild-type enzyme). $\Delta G_a$, $\Delta G_b$, $\Delta G_c$, and $\Delta G_d$ are the changes in apparent free energies of binding for the conversion of each alanine side chain to the wild-type side chain.

terms, $\Delta G_d = \Delta G_a + \Delta\Delta G_{int}$. Consequently, $\Delta\Delta G_{int}$ can be calculated from the difference between $\Delta G_a$ and $\Delta G_d$. If there is synergistic coupling between the side chains of K230 and K233, $\Delta\Delta G_{int}$ will be negative; if the coupling is antisynergistic, $\Delta\Delta G_{int}$ will be positive; and if there is no interaction between K230 and K233 side chains, then $\Delta\Delta G_{int}$ will equal zero. It should be noted that $\Delta\Delta G_{int}$ represents an energetic interaction, which may be due to either direct or indirect physical interactions between the two amino acid side chains.

## RESULTS

*The 'KFGKT' Sequence Is Involved in the Initial Binding of tRNA$^{Tyr}$, but Not in the Transfer of Tyrosine to tRNA$^{Tyr}$.* To study the role of the 'KFGKT' sequence on the second step of the aminoacylation reaction, alanine variants at each position of the 'KFGKT' sequence were analyzed using presteady-state kinetic analyses (at position 231, the more conservative F231L substitution was analyzed rather than the F231A variant). Stopped-flow fluorescence was used to monitor changes in the intrinsic fluorescence of tyrosyl-tRNA synthetase on the formation of the E·[Tyr-tRNA$^{Tyr}$·AMP]$^{‡}$ complex (*27*). After correcting for inner filter effects, the intrinsic fluorescence of tyrosyl-tRNA synthetase decreased by 10% during the transfer of tyrosine to tRNATyr (data not shown). No fluorescence changes were observed upon the initial binding of the in vitro transcribed tRNA$^{Tyr}$ substrate to the E·Tyr-AMP intermediate. These results are consistent with previous observations by Avis et al. involving in vitro transcribed tRNA$^{Tyr}$ (*27*). For each variant, the initial rates for the formation of the transition state complex were plotted against the various concentrations of the tRNA$^{Tyr}$ substrate. A rapid equilibrium assumption was applied for the tyrosine transfer step of the aminoacylation (*27*). The forward rate constants ($k_4$) and the tRNA$^{Tyr}$ dissociation ($K_d^{tRNA}$) constants were determined from a plot of initial rate vs [tRNA$^{Tyr}$] (Figure 2).

Table 1 shows the rate and dissociation constants for variants at each position in the 'KFGKT' sequence of the tyrosyl-tRNA synthetase. All of the experiments were done a minimum of 3 times with two independent tyrosyl-tRNA synthetase and tRNA$^{Tyr}$ preparations. Previous studies have shown that replacement of K230, K233, or T234 with alanine

Table 1: Binding and Rate Constants for Each of the Tyrosyl-tRNA Synthetase Variants[a]

| enzyme variant | $k_4$ ($s^{-1}$) | $K_{tRNA}$ ($\mu$M) | $k_4/K_{tRNA}$ ($\mu M^{-1}$ $s^{-1}$) |
|---|---|---|---|
| wild type | 31 ± (1) | 0.39 ± (0.03) | 81 ± (4) |
| K230A | 27 ± (1) | 2.4 ± (0.2) | 11 ± (1) |
| F231L | 28.2 ± (0.4) | 0.30 ± (0.03) | 99 ± (3) |
| G232A | 28.6 ± (0.9) | 0.36 ± (0.01) | 80 ± (1) |
| K233A | 31 ± (1) | 1.7 ± (0.1) | 18 ± (2) |
| T234A | 28.1 ± (0.1) | 0.26 ± (0.01) | 109 ± (5) |
| K230A/K233A | 29 ± (1) | 3.0 ± (0.2) | 9.8 ± (0.9) |
| Δ(227−234) | 30.9 ± (0.6) | 3.4 ± (0.2) | 9.1 ± (0.3) |

[a] Experimental errors are indicated in parentheses.

decreases the forward rate constant for the formation of enzyme-bound tyrosyl-adenylate ($k_3$) for the first step of the aminoacylation reaction by 2−3 orders of magnitude (*20*−*24*). Variants at other positions of the 'KFGKT' sequence resulted in decreases of only 2−3-fold in $k_3$ (*23*). As shown in Table 1, the forward rate constants for the transfer of tyrosine to tRNA$^{Tyr}$ ($k_4$) are not significantly affected by alanine substitutions in the 'KFGKT' sequence. In contrast, the binding of tRNA$^{Tyr}$ to the E·Tyr-AMP complex is 6−9-fold weaker for the K230A, K233A, and K230A/K233A variants than it is for the wild-type enzyme. The dissociation constants ($K_d^{Tyr}$) are unaltered in the F231L, G232A, and T234A variants. The results obtained for the wild-type tyrosyl-tRNA synthetase are identical (within experimental error) to those obtained previously by Avis et al. (*27*).

*Effects of the 'KFGKT' Sequence Variants on the Free Energy of Each Step along the Reaction Pathway*. In the first step of the aminoacylation reaction, the 'KFGKT' sequence stabilizes the E·Tyr·ATP and E·[Tyr-ATP]$^{‡}$ complexes, but is not involved in the initial binding of the tyrosine substrate to the tyrosyl-tRNA synthetase (*20*, *21*). The difference between the free energies of binding for each variant enzyme and the wild-type enzyme ($\Delta\Delta G_{app}$) in the second step of the aminoacylation reaction is shown in Figure 3. The binding of tRNA$^{Tyr}$ to the E·Tyr-AMP complex is significantly decreased in the K230A, K233A, and K230A/K233A variants relative to the wild-type enzyme ($\Delta\Delta G_{app}$ = 0.87−1.21 kcal/mol). None of the other 'KFGKT' variants exhibits a $\Delta\Delta G_{app}$ of more than 0.5 kcal/mol for the binding of tRNA$^{Tyr}$.

Previous studies have shown that the K230A, K233A, and T234A variants can destabilize the transition state complex for the first step of the aminoacylation reaction by 2.8−3.1 kcal/mol (*20*−*24*). The $\Delta\Delta G_{app}$ values for the formation of the transition state complex, E·[Tyr-tRNA$^{Tyr}$·AMP]$^{‡}$, vary between 0.88 and 1.25 kcal/mol for the K230A, K233A, and K230A/K233A variants. This is a much weaker interaction than is observed between these residues and the E·[Tyr-ATP]$^{‡}$ complex for the first step of the aminoacylation reaction. In addition, T234A, which is important for the stabilization of the transition state complex for the first step of the aminoacylation reaction ($\Delta\Delta G_{app}$ = 3.0 kcal/mol), does not have any effect on the stabilization of the transition state complex for the second step of the reaction ($\Delta\Delta G_{app}$ = −0.17 kcal/mol). None of the remaining 'KFGKT' variants display a $\Delta\Delta G_{app}$ value greater that 0.5 kcal/mol for formation of the E·[Tyr-tRNA$^{Tyr}$·AMP]$^{‡}$ complex.

*Deletion of the 'KFGKT' Sequence Indicates That K230 and K233 Are Solely Responsible for the Interaction between*

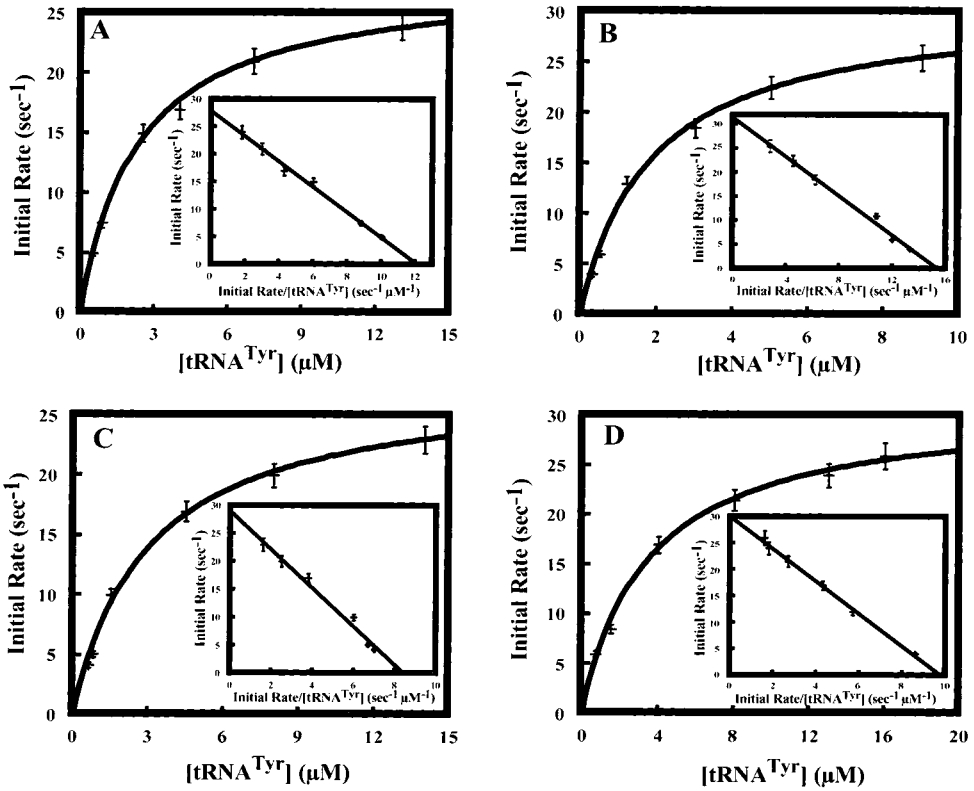


FIGURE 2: Typical Michaelis−Menten plots for the transfer of tyrosine to in vitro transcribed *B. stearothermophilus* tRNA$^{Tyr}$ substrate are shown for the following tyrosyl-tRNA synthetase variants: K230A (panel A), K233A (panel B), K230A/K233A (panel C), and the loop deletion variant Δ(227−234) (panel D). The insets are Eadie−Hoftsee transformations of the data. Michaelis−Menten plots for the wild-type tyrosyl-tRNA synthetase were similar to those observed by Avis et al. (*27*; data not shown).

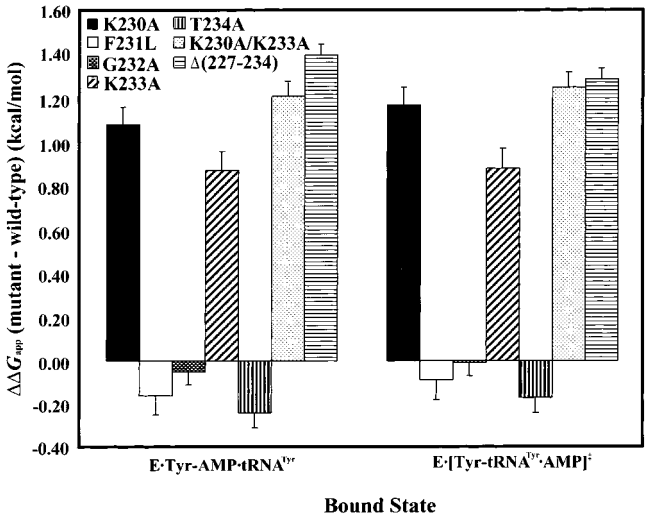


FIGURE 3: ΔΔ$G_{app}$ for the 'KFGKT' sequence variants. The differences in free energies between the complexes of the variants and the wild-type enzymes (ΔΔ$G_{app}$) are shown for each enzyme-bound state in the second step of the tRNA$^{Tyr}$ aminoacylation reaction.

*the Mobile Loop and tRNA$^{Tyr}$* . To investigate whether the effect of the 'KFGKT' sequence on the second step of the aminoacylation reaction is entirely due to the K230 and K233 side chains, a mobile loop deletion variant, Δ(227−234), was analyzed using pre-steady-state kinetic analyses. As shown in Table 1, the Δ(227−234) variant decreases the binding affinity between tRNA$^{Tyr}$ and E·Tyr-AMP by 8.7-fold. This is identical (within experimental error) to the effect that the K230A/K233A variant has on the binding affinity between tRNA$^{Tyr}$ and the E·Tyr-AMP complex. The Δ(227−234) variant also has a similar effect on the stabilization of the transition state complex for the second step of the aminoacylation reaction as that of the K230A/K233A variant. As shown in Figure 3, the transition state complex, E·[Tyr-tRNA$^{Tyr}$·AMP]$^{‡}$, is destabilized by 1.29 kcal/mol in the Δ(227−234) variant, compared to 1.30 kcal/mol for the K230A/K233A variant. These results suggest that either the peptide backbone of the 'KFGKT' sequence does not play a role in the second step of the aminoacylation reaction or, if the peptide backbone is involved in the reaction, it is replaced by the peptide backbone from other amino acid residues in the Δ(227−234) variant.

*Free Energy Profiles Indicate Replacement of K230 and K233 with Alanine Stabilizes the E·Tyr-AMP·tRNA$^{Tyr}$ and the E·[Tyr-tRNA$^{Tyr}$·AMP]$^{‡}$ Complexes to the Same Exten*t. To evaluate the contribution of the K230 and K233 amino acid residues on the reaction pathway, free energy profiles were calculated for the K230A and K233A tyrosyl-tRNA synthetase variants. As shown in Figure 4, mutation of either K230 or K233 to alanine does not affect the Gibbs activation energy for the second step of the aminoacylation reaction.

*There Is a Synergistic Coupling between K230 and K233 during the Initial Binding of tRNA$^{Tyr}$ to the E·Tyr-AMP Complex*. The effect of the energetic interaction between two amino acid residues on the stabilization of the complex for each step in the reaction pathway can be analyzed thermodynamically using double mutant free energy cycles (*21*, *24*, *33*−*35*). Figure 5 shows thermodynamic cycles for the effect that the interaction between the K230 and K233 side chains has on the initial binding of tRNA$^{Tyr}$ to E·Tyr-AMP (panel A) and on the subsequent formation of the E·[Tyr-tRNA$^{Tyr}$·

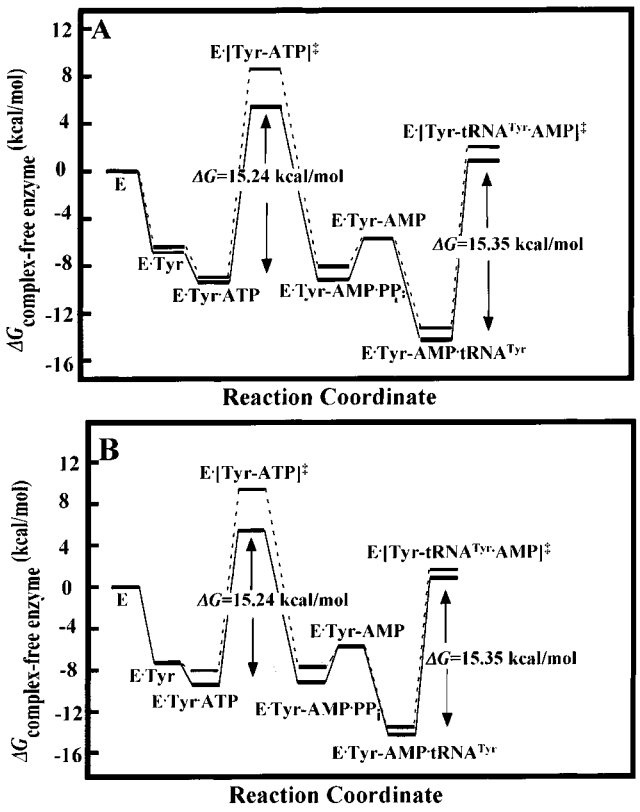


FIGURE 4: Free energy diagrams for the formation of the E·Tyr-AMP·tRNA$^{Tyr}$ and E·[Tyr-tRNA$^{Tyr}$·AMP]‡ complexes. Solid lines indicate the free energy changes during the course of the reaction for the wild-type tyrosyl-tRNA synthetase. Dashed lines indicate the effects that K230A (panel A) and K233A (panel B) have on the stability of each enzyme-bound complex in the aminoacylation reaction. Values for wild-type, K230A, and K233A variants for the first step of the aminoacylation reaction are taken from Fersht et al. (*20*) and First and Fersht (*22*).

AMP]‡ complex (panel B). In these cycles, the starting point for each cycle is the double alanine variant of the enzyme. The cycles are constructed by the sequential conversion of alanine residues to wild-type residues. It should be noted that this is the opposite frame of reference as that used for calculating the $\Delta\Delta G_{app}$ values (e.g., $\Delta G_d$ in the double mutant free energy cycle is calculated by subtracting the free energy of the wild-type enzyme from the free energy of the K230A variant). In this new frame of reference, a negative $\Delta G$ value indicates that the lysine variant is more stable than the alanine variant (e.g., $\Delta G_d = -0.88$ kcal/mol indicates the wild-type tyrosyl-tRNA synthetase is 0.88 kcal/mol more stable than the K233A variant). As shown in Figure 5, there is a pairwise interaction between the side chains of K230 and K233, which stabilizes the formation of the E·Tyr-AMP·tRNA$^{Tyr}$ and E·[Tyr-tRNA$^{Tyr}$·AMP]‡ complexes by −0.74 and −0.80 kcal/mol, respectively. These results indicate that there is a synergistic interaction between these two amino acid residues during the initial binding of the tRNA$^{Tyr}$ substrate.

## DISCUSSION

*The 'KMSKS' Motif Participates in the Initial Binding of tRNA$^{Tyr}$ to the E·Tyr-AMP Complex.* In this study, we address the question of what role the 'KMSKS' motif plays in the transfer of tyrosine to tRNA$^{Tyr}$. Previous investigations have shown that K230, K233, and T234 are located in a flexible loop in tyrosyl-tRNA synthetase and help stabilize the E·[Tyr-ATP]‡ complex, indicating that they are in the vicinity of the active site of the tyrosyl-tRNA synthetase (*20*−*24*). Hountondji et al. (*3*) observed that periodate oxidation of tRNA$^{Tyr}$ results in the formation of covalent cross-links between adenosine 76 of the tRNA$^{Tyr}$ substrate and lysines 225, 230, and 233 in tyrosyl-tRNA synthetase. Based on their perioate oxidation results, Hountondji et al. hypothesized that the 'KFGKT' sequence interacts with the 3′ end of tRNA$^{Tyr}$ (*3*). This hypothesis is consistent with the observation that the 'KFGKT' sequence stabilizes the pyrophosphate moiety of ATP during formation of the E·[Tyr-ATP]‡ complex for the first step of the aminoacylation reaction (i.e., tyrosine activation) and is therefore in the proximity of the 3′ end of tRNA$^{Tyr}$. Based on the above observations and the conserved nature of the 'KMSKS' motif in all Class I aminoacyl-tRNA synthetases, we hypothesized that the 'KFGKT' sequence in tyrosyl-tRNA synthetase may play a catalytic role in the second step of the aminoacylation reaction (i.e., the transfer of tyrosine to tRNA$^{Tyr}$), with the lysine residues of the 'KFGKT' sequence forming electrostatic interactions with the negatively charged phosphate groups of adenosine 76 in tRNA$^{Tyr}$. This hypothesis was tested by analyzing the effects that replacing each amino acid in the 'KFGKT' sequence with alanine (or leucine in the case of F231) has on the formation of the E·[Tyr-tRNA$^{Tyr}$·AMP]‡ complex. Pre-steady-state kinetic analyses indicate that while replacement

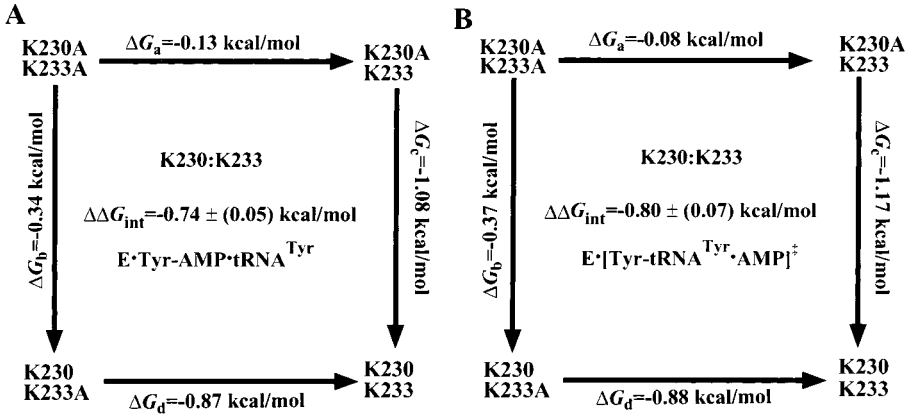


FIGURE 5: Double mutant free energy cycles for the pairwise coupling between the side chains of K230 and K233. The double mutant free energy cycles for the interaction of side chains of K230 and K233 (relative to alanine) are shown for the E·Tyr-AMP·tRNA$^{Tyr}$ (panel A) and E·[Tyr-tRNA$^{Tyr}$·AMP]‡ (panel B) complexes. The free energy of interaction, $\Delta\Delta G_{int}$, is calculated by subtracting the changes in free energy for opposing sides of the cycle (e.g., $\Delta\Delta G_{int} = \Delta G_d - \Delta G_a$).

of amino acids K230 and K233 with alanine decreases the binding affinity between the enzyme and $tRNA^{Tyr}$, the stability of the E·[Tyr-$tRNA^{Tyr}$·AMP]‡ complex relative to the E·Tyr-AMP·$tRNA^{Tyr}$ complex is unaffected by replacement of the lysine residues with alanine. In addition, the interaction between the 'KFGKT' sequence and $tRNA^{Tyr}$ differs significantly from the interaction between the 'KFGKT' sequence and ATP in the E·[Tyr-ATP]‡ complex. In the E·[Tyr-ATP]‡ complex, K230, K233, and T234 all make relatively strong interactions (2.8−3.1 kcal/mol) with the ATP moiety (*21*−*23*), whereas in the E·Tyr-AMP·$tRNA^{Tyr}$ complex, only K230 and K233 interact with $tRNA^{Tyr}$, and these interactions are relatively weak (0.9−1.2 kcal/mol). Finally, in the E·[Tyr-ATP]‡ complex, there is a substantial interaction between the K230, K233, and T234 side chains (*24*), which helps stabilize the E·[Tyr-ATP]‡ complex. Based on this observation, we hypothesized that there is a synergistic interaction between K230 and K233 in the E·Tyr-AMP·$tRNA^{Tyr}$ complex. Double mutant free energy cycle analysis supports this hypothesis. Thus, while the hypothesis that the 'KFGKT' sequence plays a catalytic role in the tyrosine transfer step of the tRNA aminoacylation reaction appears to be incorrect, this sequence does stabilize the initial binding of the $tRNA^{Tyr}$ substrate. The data presented in this paper are the first kinetic evidence that the 'KFGKT' sequence participates in the initial binding of $tRNA^{Tyr}$ to tyrosyl-tRNA synthetase.

*Mechanistic Interpretation of the Role That the 'KFGKT' Motif Plays in the Tyrosine Transfer Step of the $tRNA^{Tyr}$ Aminoacylation Reaction*. The 'KFGKT' motif in tyrosyl-tRNA synthetase has been the subject of extensive studies for the first step of the $tRNA^{Tyr}$ aminoacylation reaction (i.e., tyrosine activation). The role of the 'KFGKT' sequence in the catalytic mechanism of tyrosyl-tRNA synthetase has now been investigated from the initial binding of the tyrosine substrate to the enzyme, through the transfer of the tyrosine substrate to $tRNA^{Tyr}$. Based on the data presented in this paper, as well as previous investigations (*20*−*24*), we propose the following model for the role of the 'KFGKT' sequence during catalysis of $tRNA^{Tyr}$ aminoacylation. Initially, the 'KFGKT' sequence is situated at least 10 Å away from the active site of the enzyme on a flexible loop (*5*, *6*). On the binding of ATP to the enzyme, the 'KFGKT' sequence moves toward the active site of the enzyme, where it interacts with the ATP substrate, preventing it from binding too tightly to the enzyme (i.e., it prevents the E·Tyr·ATP complex from falling into a "thermodynamic well" which would increase the activation energy for the E·[Tyr-ATP]‡ complex) (*23*, *24*). The interaction between the 'KFGKT' sequence and the pyrophosphate groups of ATP increases as the E·[Tyr-ATP]‡ complex forms, and then weakens as the bond between the α- and *β*-phosphates of ATP is broken (*20*−*24*). Release of the pyrophosphate moiety from E·[Tyr-AMP·$PP_i$] results in the return of the 'KFGKT' sequence to its original position (i.e., 10 Å away from the active sites of the enzyme). This increases the accessibility of the active site to $tRNA^{Tyr}$. Based on the results presented in this paper, one of two scenarios occurs during the initial binding of $tRNA^{Tyr}$. In the first scenario, the binding of $tRNA^{Tyr}$ is accompanied by the 'KFGKT' sequence moving back toward the active site and forming weak interactions with adenosine 76 of the $tRNA^{Tyr}$ substrate. The 'KFGKT' sequence continues to interact with adenosine 76 during formation of the E·[Tyr-$tRNA^{Tyr}$·AMP]‡ complex, although the strength of this interaction does not change during formation of this transition state complex. This mechanism is consistent with the model proposed by Bedouelle and colleagues (*36*−*38*) for the interaction of tyrosyl-tRNA synthetase with $tRNA^{Tyr}$. In their model, the only nucleotide in $tRNA^{Tyr}$ that the 'KFGKT' sequence is positioned to interact with is adenosine 76, and even this interaction requires that the 'KFGKT' sequence moves 5−10 Å toward the active site of the enzyme. In the other scenario, the 'KFGKT' sequence remains 10 Å away from the active site when $tRNA^{Tyr}$ binds and does not interact with adenosine 76. Instead, the 'KFGKT' sequence on the other subunit of tyrosyl-tRNA synthetase (i.e., the subunit that recognizes the $tRNA^{Tyr}$ anticodon) interacts with the variable stem and loop of $tRNA^{Tyr}$, thereby stabilizing the initial binding of $tRNA^{Tyr}$. Preliminary modeling of the docking between $tRNA^{Phe}$ and tyrosyl-tRNA synthetase supports this latter model (Xin and Dwyer, unpublished results). Experiments are currently underway to distinguish these two models.

## CONCLUSIONS

The amino acid side chains of K230 and K233 in the 'KFGKT' sequence of tyrosyl-tRNA synthetase have been found to stabilize the initial binding of $tRNA^{Tyr}$ to the E·Tyr-AMP complex, but do not play a catalytic role in the transfer of tyrosine to the $tRNA^{Tyr}$ substrate. Stabilization of the E·[Tyr-AMP·$tRNA^{Tyr}$] complex involves synergistic coupling between the side chains of K230 and K233. The results presented in this paper provide the first kinetic evidence that the 'KMSKS' motif in Class I aminoacyl-tRNA synthetases participates in the initial binding of $tRNA^{Tyr}$ to tyrosyl-tRNA synthetase.

## ACKNOWLEDGMENT

We thank Professor Alan Fersht for the pGAG2 and pAR1219 plasmids and Dr. George Garcia for the *E. coli* TG2 strain; Dr. Donard Dwyer for assistance in modeling the TyrRS·$tRNA^{Phe}$ complex; Dongbing Wei and Keith Simpson for technical services during the initial stages of this research; and Dr. Sergey Slepenkov for assistance on the stopped-flow spectrophotometer.

## REFERENCES

1. Eriani, G., Delarue, M., Poch, O., Gangloff, J., and Moras, D. (1990) *Nature 347*, 203−206.
2. Moras, D. (1992) *Trends Biochem. Sci. 17*, 159−164.
3. Hountondji, C., Dessen, P., and Blanquet, S. (1986) *Biochimie 69*, 1071−1078.
4. Webster, T., Tsai, H., Kula, M., Mackie, G. A., and Schimmel, P. (1984) *Science 226*, 1315−1317.
5. Brick, P., and Blow, D. M. (1987) *J. Mol. Biol. 194*, 287−297.
6. Brick, P., Bhat, T. N., and Blow, D. M. (1989) *J. Mol. Biol. 208*, 83−98.
7. Brunie, S., Zelwer, C., and Risler, J. L. (1990) *J. Mol. Biol. 216*, 411−424.
8. Edwards, H., Trezeguet, V., and Schimmel, P. (1991) *Proc. Natl. Acad. Sci. U.S.A. 88*, 1153−1156.
9. Rould, M. A., Perona, J. J., and Steitz, T. A. (1991) *Nature 352*, 213−218.
10. Zelwer, C., Risler, J. L., and Brunie, S. (1982) *J. Mol. Biol. 155*, 63−81.

11. Walker, J. E., Saraste, M., Runswick, M. J., and Gay, N. J. (1982) *EMBO J. 1*, 945−951.
12. Walker, J. E., Saraste, M., and Gay, N. J. (1984) *Biochim. Biophys. Acta 768*, 164−200.
13. Cusack, S., Berthet-Colominas, C., Hartlein, M., Nassar, N., and Leberman, R. (1990) *Nature 347*, 249−255.
14. Delarue, M., and Moras, D. (1993) *Bioessays 15*, 675−687.
15. Carter, P., Bedouelle, H., and Winter, G. (1986) *Proc. Natl. Acad. Sci. U.S.A. 83*, 1189−1192.
16. Fersht, A. R. (1975) *Biochemistry 14*, 5−12.
17. Jones, D. H., McMillan, A. J., Fersht, A. R., and Winter, G. (1985) *Biochemistry 24*, 5852−5857.
18. Ward, W. H., and Fersht, A. R. (1988) *Biochemistry 27*, 5525−5530.
19. Ward, W. H., and Fersht, A. R. (1988) *Biochemistry 27*, 1041−1049.
20. Fersht, A. R., Knill-Jones, J. W., Bedouelle, H., and Winter, G. (1988) *Biochemistry 27*, 1581−1587.
21. First, E. A., and Fersht, A. R. (1993) *Biochemistry 32*, 13644−13650.
22. First, E. A., and Fersht, A. R. (1993) *Biochemistry 32*, 13651−13657.
23. First, E. A., and Fersht, A. R. (1993) *Biochemistry 32*, 13658−13663.
24. First, E. A., and Fersht, A. R. (1995) *Biochemistry 34*, 5030−5043.
25. Gibson, T. A. (1984) Ph.D. Thesis, University of Cambridge, Cambridge, U.K.
26. Wilkinson, A. J., Fersht, A. R., Blow, D. M., and Winter, G. (1983) *Biochemistry 22*, 3581−3586.
27. Avis, J. M., Day, A. G., Garcia, G. A., and Fersht, A. R. (1993) *Biochemistry 32*, 5312−5320.
28. Zhang, S. B., Bronskill, P. M., Wang, Q. S., and Wong, J. T. (1986) *J. Chromatogr. 360*, 282−287.
29. Rassi, Z. E., and Horvath, C. (1985) *J. Chromatogr. 360*, 79−90.
30. Pleiss, J. A., Maria, L. D., and Uhlenbeck, O. C. (1998) *RNA 4*, 1313−1317.
31. England, T. E., and Uhlenbeck, O. C. (1978) *Nature 275*, 560−561.
32. McSwiggen, J. A. (1991) *Comments 17*, 1−8.
33. Carter, P. J., Winter, G., Wilkinson, A. J., and Fersht, A. R. (1984) *Cell 38*, 835−840.
34. Horovitz, A. (1987) *J. Mol. Biol. 196*, 733−735.
35. Horovitz, A., and Fersht, A. R. (1992) *J. Mol. Biol. 224*, 733−740.
36. Bedouelle, H. (1990) *Biochimie 72*, 589−598.
37. Bedouelle, H., Guez-Ivanier, V., and Nageotte, R. (1993) *Biochimie 75*, 1099−1108.
38. Bedouelle, H., and Winter, G. (1986) *Nature 320*, 371−373.

BI991675L